High-energy, high-repetition-rate picosecond pulses from a quasi-CW diode-pumped Nd:YAG system

Daniel W. E. Noom,* Stefan Witte, Jonas Morgenweg, Robert K. Altmann, and Kjeld S. E. Eikema

LaserLaB Amsterdam, VU University Amsterdam, De Boelelaan 1081, 1081 HV Amsterdam, The Netherlands

**Corresponding author: d.w.e.noom@vu.nl*

Received June 10, 2013; revised July 6, 2013; accepted July 15, 2013; posted July 17, 2013 (Doc. ID 191957); published August 7, 2013

We report on a high-power quasi-CW pumped Nd:YAG laser system, producing 130 mJ, 64 ps pulses at 1064 nm wavelength with a repetition rate of 300 Hz. Pulses from a Nd:YVO_4 oscillator are first amplified by a regenerative amplifier to the millijoule level and then further amplified in quasi-CW diode-pumped Nd:YAG modules. Pulsed diode pumping enables a high gain at repetition rates of several hundred hertz, while keeping thermal effects manageable. Birefringence compensation and multiple thermal-lensing-compensated relay-imaging stages are used to maintain a top-hat beam profile. After frequency doubling, 75 mJ pulses are obtained at 532 nm. The intensity stability is better than 1.1%, which makes this laser an attractive pump source for a high-repetition-rate optical parametric amplification system.

OCIS codes: (140.3280) Laser amplifiers; (140.3480) Lasers, diode-pumped; (140.3580) Lasers, solid-state; (140.3530) Lasers, neodymium.

http://dx.doi.org/10.1364/OL.38.003021

High-energy ultrashort laser pulses are used in high-harmonic generation schemes for the production of coherent radiation in the ultraviolet and soft x-ray spectral region [1]. These pulses can be produced with optical parametric chirped pulse amplification (OPCPA) [2], which is particularly suited for the generation of intense few-cycle pulses. OPCPA combines the high energy of long, narrowband pump pulses with the broadband spectrum of ultrashort seed pulses.

The main challenge in OPCPA development is the relatively high technical demands placed on the pump laser. The pump pulse duration should be matched to that of the stretched seed pulse [2], which is typically in the picosecond range, as excessive pulse stretching results in problems with low seed intensity, and complicates recompression. At the same time, both a high pulse energy and high repetition rate are desirable for many experiments.

High-energy pump pulses are generally produced in a master-oscillator power-amplifier scheme, where the generation of pulses is decoupled from the high-power amplification. Amplifier construction depends on the properties of the used gain materials, such as Nd- or Yb-doped crystals. Yb:YAG has gained a lot attention lately because of its favorable properties as a gain material. It has a high saturation fluence, and cryogenic cooling improves thermal conductivity and also transforms this medium from a quasi-three-level to a more favorable four-level system. Yb:YAG has been used in Innoslab [3], disk [4,5] and rod [6,7] schemes. Yb has also been used in different host materials, such as Yb:GSAG [8] and Yb:YLF [9] to increase the gain bandwidth.

Nd:YAG on the other hand is a well-established material that has been widely used in flashlamp-pumped cylindrical rod amplifiers. However, the repetition rate of such systems has typically been limited to the 10 Hz range [10,11], due to both the excessive thermal load and the limited number of shots before degradation of the flashlamps. New developments in laser diode engineering have made it possible to use quasi-continuously (QCW) pumping diodes in amplification modules. These QCW diodes enable a much more efficient pumping as they can be turned off between consecutive pulses. This strongly reduces the thermal load on the gain medium while preserving a high gain. As a result, the repetition rate can be increased by more than an order of magnitude.

In this paper we report our results on a quasi-CW diode pumped, Nd:YAG based amplification system that delivers 75 mJ, 64 ps pulses at a wavelength of 532 nm and a repetition rate of 300 Hz. For homogeneous amplification in the OPCPA, and to maximize energy extraction, a top-hat beam profile is implemented. Thermal birefringence compensation is used in combination with relay imaging to generate this beam profile with a flat wavefront at 1064 nm, resulting in efficient frequency doubling after amplification. The total footprint of the laser system is less than 1.8 m^2.

The setup is shown in Fig. 1. First, pulses are generated in a home-built Nd:YVO_4 oscillator, pumped with an 18 W, 880 nm CW diode laser. A semiconductor saturable absorber mirror inside the laser cavity ensures passive mode locking. The oscillator provides 60 nJ, 10 ps pulses at 80 MHz repetition rate at 1064 nm wavelength. After reducing the energy to 1 nJ to lower the background output of unamplified pulses, the output is used to seed a regenerative amplifier.

Inside the regenerative amplifier a Nd:YAG rod is pumped with CW laser diodes. A Pockels cell is switched on at 300 Hz, for a duration of 500 ns, to keep a single pulse traveling in the cavity for amplification in 60 round trips. A 0.5 mm thick intracavity etalon stretches the pulses in the regenerative amplifier to 64 ps, to reduce the peak intensity and to match the stretched pulse length from a Ti:sapphire oscillator which will later be used to seed an OPCPA system.

The 1.2 mJ output pulses of the regenerative amplifier are amplified in two modules from the REA-series

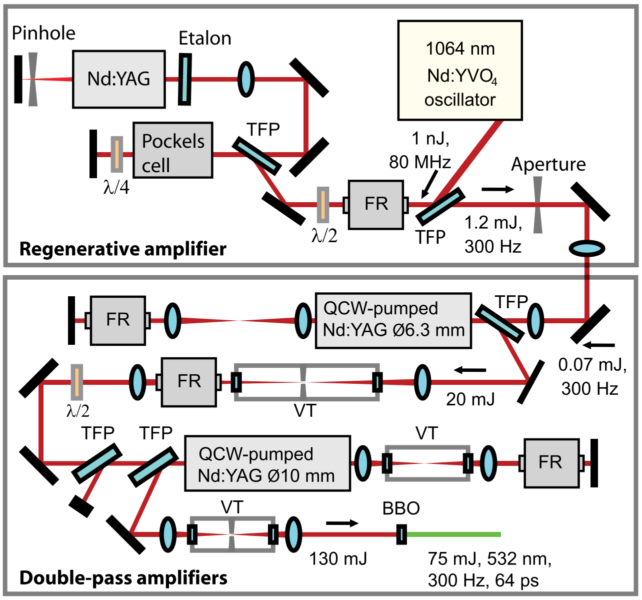

Fig. 1. Schematic of the developed Nd:YAG regenerative amplifier and quasi-CW-pumped postamplifier system. TFP, thin-film polarizer; $\lambda/2$, half-wave plate; $\lambda/4$, quarter-wave plate; FR, Faraday rotator; VT, vacuum tube.

manufactured by Northrop Grumman, containing QCW diode-pumped Nd:YAG rods. The first module has a cylindrical rod of 6.35 mm diameter and 146 mm length. Five rows of 24 diode bars are placed around the rod. The operating voltage of the diodes is 240 V and the maximum possible peak drive current is 145 A. It is operated at 85.5 A for 245 μs for each pulse, which matches the upper state lifetime of the Nd:YAG gain medium. In the second module the rod diameter is 10 mm. This module has a maximum possible current of 175 A, but it is also operated at 85.5 A.

Before seeding the double-pass amplifiers, two cylindrical lenses reduce astigmatism from the output of the regenerative amplifier. To produce a flat intensity profile in the modules, the beam is increased in size by a telescope before it is passed through a 5.5 mm aperture. This reduces the pulse energy to 0.07 mJ. The beam at the aperture is then relay-imaged inside the Nd:YAG rod of the first module. We define the front (end) face of the modules as the side where the incoming beam first enters (exits) a module. After the beam exits the first module at the end face, it is relay-imaged onto a mirror and then relay-imaged inside the rod again. This is done to preserve the flat intensity profile at the modules and at the Faraday rotators, which are used to compensate thermal birefringence (discussed in more detail below). After double-passing the first module, the beam reflects off a thin film polarizer (TFP) and is relay-imaged onto the end face of the second module. In the focus between the image planes a 3 mm diameter aperture is used to block back reflections, and from there on vacuum tubes are used to avoid nonlinear effects in air at locations where the beam is focused. In our current setup, the total gain of the modules is 2×10^3, and thus the total extinction ratio of the TFPs should be at least $\sim 10^3$ to prevent damage to optics. For this reason, two polarizers are used in front of the last Nd:YAG module.

Heating of the crystal rods by the pump diodes, combined with surface cooling, leads to a nonuniform temperature distribution inside the rods. The resulting thermal-stress-induced birefringence has radially and tangentially directed principal axes [12]. This results in beam profile deformations after interaction with optics with a polarization-dependent reflectivity. When the beam travels the same path through the rod twice with a 90 deg polarization rotation in between, both the radial and tangential polarization will have traveled the same optical path length, which compensates thermal birefringence effects [13]. This principle is implemented through a Faraday rotator in the imaging setup behind each module. The compensation is optimized by moving the position of the end mirror in this setup. From test experiments, we find that the end face of a module should be relay-imaged onto itself for optimal compensation.

The radial variation of the refractive index in the crystal rods is temperature- and stress-dependent, and together with end-face bulging this causes the rods to act as a lens. This lensing effect is mitigated by placing the lenses in each imaging setup closer together than would be required in a standard 4f relay-imaging setup.

After passing through the entire amplifier system, pulses of 130 mJ are produced at 1064 nm. We limit the pulse energy at this value to reduce the risk of damage to the Nd:YAG rods and end-face coatings. Pulses at 532 nm wavelength are generated by second-harmonic generation (SHG) in a $14 \times 14 \times 3$ mm^3 BBO crystal. Figure 2 shows the resulting energy per pulse at 532 nm for different 1064 nm pulse energies. The conversion efficiency at an input pulse energy of 130 mJ is 58%. We characterized the stability of the system by measuring the pulse-to-pulse fluctuations of both the input and amplified output pulses. We find that both are stable within 1.1% rms, which is an upper bound, as the measurement was limited by electronic noise in the detection system. Furthermore, we have performed energy stability measurements over longer time scales, and find that the output remains stable to within 1.2% rms over several tens of minutes of continuous operation. An autocorrelation trace is shown in Fig. 3. The measured autocorrelation fits very well to a Gaussian curve, and from this fit we derive a pulse length of 64 ps.

Because a flat gain profile in the OPCPA is desirable and damage depends mostly on the peak intensity, it is imperative that a flat intensity profile is maintained at critical surfaces. The top-hat beam profile will be

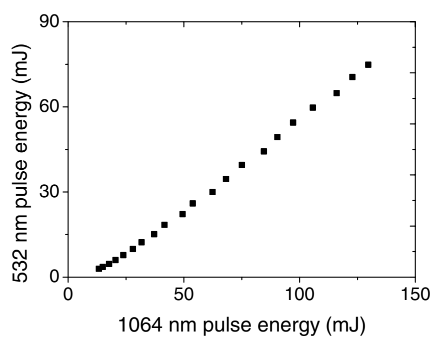

Fig. 2. Output pulse energy at 532 nm after SHG plotted against the 1064 nm input pulse energy.

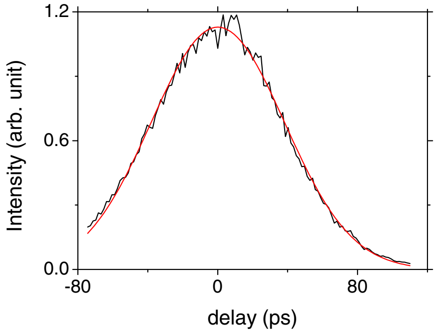

Fig. 3. Measured autocorrelation trace and Gaussian fit. The fit has a FWHM of 90 ps, which indicates a pulse length of 64 ps for a Gaussian temporal profile.

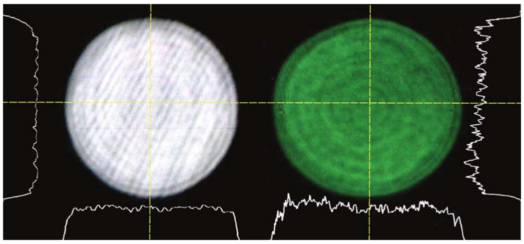

Fig. 4. Transverse beam profiles of the amplified pulses at 1064 nm (left) and after frequency doubling to 532 nm (right), measured at the position of the BBO crystal via relay imaging. Single-line cross sections at the dashed lines are included. Note that the diagonal fringes in the 1064 nm image are an artefact, due to interferences in the CCD camera. Some spots are visible in the 532 nm beam, which are caused by dust particles on neutral gray filters and the CCD itself.

distorted when it passes through apertures away from the image planes. Since the rods are transversely pumped, the homogeneity of amplification depends on how well the pump spectrum is absorbed in Nd:YAG. This spectrum, and therefore the absorption, depends on the temperature of the diodes. When this temperature is optimized for maximum absorption, the amplified beam profile shows a dip in the center. In the final design, the temperature of the diodes was adjusted in combination with the driving current to the laser diodes to increase the absorption length and homogenize the transverse gain profile in the amplifier. We measured the infrared beam profile (without SHG) and the green beam profile separately with imaging setups when the system was running at full power. Good quality top-hat beam profiles are obtained in both cases, as can be seen from Fig. 4.

To conclude, quasi-CW diode pumping provides the efficiency required to effectively use Nd:YAG as a gain material at high repetition rates. The high pulse energies and repetition rate of this system are ideal for pumping high-intensity few-cycle OPCPA. Such OPCPA systems, in turn, are an excellent starting point for high-flux generation of soft x rays. Cryogenics are avoided, which results in a fairly simple setup compared to Yb:YAG systems. The power, stability, and transverse beam profile all reach the requirements needed to pump a high-power optical parametric amplification system.

The authors gratefully acknowledge financial support by the Netherlands Organization for Scientific Research (NWO) through a NWO-groot grant and NWO Veni grant 680-47-402 and the EC via FP7 JRA INREX and BIOPTICHAL.

References

1. M.-C. Chen, P. Arpin, T. Popmintchev, M. Gerrity, B. Zhang, M. Seaberg, D. Popmintchev, M. M. Murnane, and H. C. Kapteyn, Phys. Rev. Lett. **105**, 173901 (2010).
2. S. Witte, R. T. Zinkstok, A. L. Wolf, W. Hogervorst, W. Ubachs, and K. S. E. Eikema, Opt. Express **14**, 8168 (2006).
3. M. Schulz, R. Riedel, A. Willner, T. Mans, C. Schnitzler, P. Russbueldt, J. Dolkemeyer, E. Seise, T. Gottschall, S. Hädrich, S. Duesterer, H. Schlarb, J. Feldhaus, J. Limpert, B. Faatz, A. Tünnermann, J. Rossbach, M. Drescher, and F. Tavella, Opt. Lett. **36**, 2456 (2011).
4. J. Tümmler, R. Jung, H. Stiel, P. V. Nickles, and W. Sandner, Opt. Lett. **34**, 1378 (2009).
5. A. H. Curtis, B. A. Reagan, K. A. Wernsing, F. J. Furch, B. M. Luther, and J. J. Rocca, Opt. Lett. **36**, 2164 (2011).
6. S. Klingebiel, C. Wandt, C. Skrobol, I. Ahmad, S. A. Trushin, Z. Major, F. Krausz, and S. Karsch, Opt. Express **19**, 5357 (2011).
7. K.-H. Hong, J. T. Gopinath, D. Rand, A. M. Siddiqui, S.-W. Huang, E. Li, B. J. Eggleton, J. D. Hybl, T. Y. Fan, and F. X. Kärtner, Opt. Lett. **35**, 1752 (2010).
8. D. A. Rand, S. E. J. Shaw, J. R. Ochoa, D. J. Ripin, A. Taylor, T. Y. Fan, H. Martin, S. Hawes, J. Zhang, S. Sarkisyan, E. Wilson, and P. Lundquist, Opt. Lett. **36**, 340 (2011).
9. D. E. Miller, L. E. Zapata, D. J. Ripin, and T. Y. Fan, Opt. Lett. **37**, 2700 (2012).
10. F. Tavella, A. Marcinkevicius, and F. Krausz, Opt. Express **14**, 12822 (2006).
11. S. Witte, R. T. Zinkstok, W. Hogervorst, and K. S. E. Eikema, Opt. Express **13**, 4903 (2005).
12. W. Koechner, *Solid-State Laser Engineering (Springer Series in Optical Sciences)* (Springer, 1999).
13. Q. Lü, N. Kugler, H. Weber, S. Dong, N. Müller, and U. Wittrock, Opt. Quantum Electron. **28**, 57 (1996).